J. Biochem. 132, 257–263 (2002)

Effect of Organic Anions on the Photoreaction of Photoactive Yellow Protein[1]

Nobutaka Shimizu, Hironari Kamikubo, Ken'ichi Mihara, Yasushi Imamoto, and Mikio Kataoka[2]

Department of Materials Science, Nara Institute of Science and Technology, Ikoma, Nara 630-0101

Received March 26, 2002; accepted May 24, 2002

In order to clarify changes in the structure and surface properties of photoactive yellow protein (PYP) upon light absorption, the spectroscopic properties and solution structure of its photo-intermediate (PYP_M) were examined in the presence of various anions. At identical ionic strengths, citrate slowed the decay rate of PYP_M more than acetate. Although the absorption spectrum in the dark was not affected by organic anions, citrate induced a 5-nm blue shift of the absorption maximum for PYP_M. Solution X-ray scattering experiments indicated that the radius of gyration (*Rg*) and apparent molecular weight in the dark were constant in all buffer systems. However, the *Rg* of PYP_M in citrate buffer at high concentration was 16.2 (± 0.2) Å, while the *Rg* of PYP_M in acetate buffer was 15.6 (± 0.2) Å. The apparent molecular weight increased 7% upon PYP_M formation in citrate buffer at high concentration compared to other conditions. These results suggest that citrate molecules specifically bind to PYP_M. A cluster of basic amino acid residues with a hydrogen bond donor would be exposed upon PYP_M formation and responsible for the specific binding of citrate.

Key words: photoreaction, photoreceptor, spectroscopy, structural change, X-ray scattering.

Photoactive yellow protein (PYP), a soluble photoreceptor protein for negative phototaxis of *Ectothiorhodospira halophila* (*1, 2*), has been studied as a model system of receptor proteins. PYP is a novel type of receptor protein that contains *p*-coumaric acid as the chromophore. High-resolution crystal structure studies indicate that PYP is a typical α/β protein (*3–6*) and contains a PAS domain, a sequence motif conserved among sensing and signal transduction proteins (*7–10*).

PYP is composed of 125 amino acids and *p*-coumaric acid covalently bound to Cys69 (*3, 11–13*). The photoreaction cycle of PYP has been identified by time-resolved spectroscopy and low-temperature spectroscopy (*14–22*). Among the intermediates, PYP_M (also called I_2 or pB) has an extremely blue-shifted spectrum (λ_{max} ~ 360 nm) due to the protonation of the chromophore, for which Glu46 is a proton donor (*22, 23*). PYP_M returns to the original state in about 500 ms at room temperature under neutral pH. PYP_M is considered to be a physiologically active state.

It is expected that tertiary structural changes alter the surface structure upon the formation of PYP_M, resulting in binding to a downstream transducer. Several lines of evidence suggest a conformational change in PYP occurs upon light absorption. Multidimensional NMR measurements demonstrated the loss of some signals, suggesting the conformation around the N terminal domain is highly disordered (*24, 25*). Thermodynamic studies suggest that the hydrophobic domain buried inside the protein in a dark state is exposed to solvent during the formation of PYP_M (*15, 26*). Conformational changes in the main chain have been shown by FTIR (*27–30*). In contrast, the crystal structure of PYP_M revealed by time-resolved Laue diffraction shows no large conformational changes (*4*). The change is confined to the vicinity of the chromophore. These findings make it necessary to conduct structural studies of PYP_M in solution to understand the surface properties responsible for target recognition and binding.

Our previous study about urea-induced unfolding of PYP and PYP_M showed that the stability of PYP_M is affected by the buffer system, while that of PYP is not (*31*). Citrate buffer stabilizes PYP_M against urea more than acetate buffer. This result suggested the possibility of a specific interaction of citrate molecules with PYP_M. The surface property change in PYP_M should be involved in the downstream signaling if a target molecule interacts with the photolyzed PYP. In order to elucidate the surface properties and structural changes during PYP_M formation, we examined the effect of various anions, including citrate, on the photoreaction and the solution structure of PYP_M using UV-visible spectroscopic and solution X-ray scattering methods. The results showed the specific interaction between PYP_M and some species of organic anion molecules, causing a prolongation of the lifetime of PYP_M. The solution structure is swollen during PYP_M formation, and an extra structural

[1] This work was partly supported by a Grant-in-Aid from the Ministry of Education, Culture, Sports, Science and Technology of Japan to M.K. and H.K.

[2] To whom correspondence should be addressed. Phone: +81-743-72-6100, Fax: +81-743-72-6109, E-mail: kataoka@ms.aist-nara.ac.jp

Abbreviations: PYP, photoactive yellow protein; PYP_M, the M intermediate of PYP; λ_{max}, absorption maximum in the visible region; $I(0)$, a scattering intensity at $\theta = 0$; $I(0)/c$, $I(0)$ divided by the weight concentration; *Rg*, radius of gyration; $[I(0)/c]_{conc \to 0}$, evaluated by the extrapolation to 0 protein concentration.

change was also observed in the anion-bound form of PYP_M. The configuration and number of charges on acidic molecules are critical to the specific binding to PYP_M. On the basis of these results, we will discuss a model for the surface property change in PYP_M.

MATERIALS AND METHODS

Purification of PYP—Apo-PYP was overexpressed in *Escherichia coli* BL21(DE3) (Novagen) and solubilized with urea, as reported previously (*32*). Holo-PYP was reconstituted by adding *p*-coumaric anhydride to apo-PYP (*32*). PYP was purified by DEAE-Sepharose column chromatography. The final purity index value (A_{279}/A_{446}) was 0.44. The purified PYP was dialyzed against the buffers described below. PYP was concentrated on an ultrafiltration membrane (Centricon YM10, Millipore). All procedures were performed under red light.

Buffers—The buffer systems used were citrate–citrate Na, 1,2,3-propane-tricarboxylate–1,2,3-propane-tricarboxylate Na, glutarate–glutarate Na, and acetate–acetate Na. The concentration of each buffer varied between 1 mM and 1 M. The effects of chloride and sulfate were examined in 10 mM acetate buffer containing NaCl (1 mM–1 M) or Na_2SO_4 (1 mM–1 M). The pH of the sample solution was adjusted to pH 5.0 at 5°C. In water, ionic strength, μ, is generally described by the concentration of each ion in solution, c, and the electric charge number of the ion, z, as

$$\mu = \frac{1}{2}\sum c_i z_i^2,$$

where i denotes the ion species. Therefore, the resulting value is obtained by the summation of all types of ions in solution. In our experiments, weak acidic reagents were used. Several species with different numbers of charges derived from multivalent acidic molecules are in a balanced state. To calculate the ionic strength, the concentration of each species at 5°C, pH 5.0, was evaluated using the Henderson-Hasselbalch equation. The values of pK_a, ratios of the coexistent species, and effective charge for each weak acidic molecule used here are summarized in Table I.

Spectroscopy—UV-visible spectroscopy was carried out with a UV2400 spectrophotometer (SHIMADZU). The temperature of the sample cell was kept at 5°C using an RTE-111 coolnics circulator (NESLAB Instruments). The excitation light was introduced from the top of the cell by an LA-60Me (60 W) cold light source (Hayashi Watch Engineering) through a Y43 glass filter (Asahi Techno Glass). UV-D36A glass filters (Asahi Techno Glass) (300 nm < λ < 390 nm) were placed in front of the detector windows of the spectrophotometer to protect the detector from the excitation light.

Solution X-Ray Scattering—Solution X-ray scattering measurements were carried out at BL-10C, Photon Factory, Tsukuba (*33, 34*). The wavelength of the X-rays was adjusted to 1.488 Å with a Si monochrometer. The scattering intensities $I(q)$ were recorded with a one-dimensional detector, PSPC (RIGAKU), with a 4 mm aperture slit, where $q = 4\pi\sin\theta/\lambda$ is scattering vector, 2θ is scattering angle, and λ is wavelength of the X-rays. In a very small angle region, $I(q)$ can be approximated by the following equation:

$$I(q) = I(0)\exp[-Rg^2(q^2/3)],$$

where $I(0)$ is scattering intensity at $\theta = 0$ and Rg is the radius of gyration (*35, 36*). Therefore, the slope and Y-intersection of ln $I(q)$ *versus* q^2 give $-Rg^2/3$ and ln $I(0)$, respectively.

The exposure time was 5 min. Three to five sets of independent measurements were averaged to improve the signal-to-noise ratio. The protein concentration was varied from 4 to 12 mg/ml. The excitation light (HILUX-HR slide projector lamp, Tokyo Master) through a Y43 glass filter was directed to the sample from the side of the cell window using a small bent cylindrical mirror. The temperature of the cell was kept at 5°C.

TABLE I. **The values of pK_a, ratios of coexistent species, and effective charges for acetate (A), glutarate (G), 1,2,3-propane-tricarboxylate (P), and citrate (C) at pH 5.0, 5.0°C.**

	pK_{a1}	pK_{a2}	pK_{a3}	Valence (%)			Effective charge
				1-	2-	3-	
A	4.78	—	—	62.4	—	—	–0.62
G	4.04	5.41	—	60.9	23.7	—	–1.08
P	3.57	4.69	5.94	30.4	61.4	7.1	–1.74
C	3.2	4.82	6.39	38.6	58.4	2.4	–1.63

RESULTS

Prolongation of the Lifetime of PYP_M under Conditions of Acidic pH and High Salt Concentration—Figure 1a shows the absorption spectrum of PYP in the dark and under continuous illumination (>430 nm) in 300 mM acetate buffer at pH 5.0. The spectrum under illumination is limited to between 300 and 390 nm due to the band-pass filter that prevents exciting light from getting into the detector. The absorption spectrum in the dark was completely identical to that at neutral pH. The absorption maximum under illumination was 360 nm, indicating an accumulation of PYP_M.

Figure 1b shows the effect of acetate on the time course of the absorbance change at 350 nm before and after irradiation for 60 s (from –60 to 0 s in figure). The curves (1–5) were obtained at various concentrations of acetate using the same concentration of PYP. The intensity of the exciting light was kept constant for all spectroscopic measurements. The absorbance at 350 nm increased during illumination due to the formation of PYP_M and then decreased immediately after turning off the light due to its decay. The absorbance increase reached a plateau in 20 s, indicating that a photo-steady-state was formed. The absorbance increase at the photo-steady-state and the decrease in decay rate were in proportion to the concentration of acetate.

The Relationship between Ionic Strength and the Lifetime of PYP_M—As acetate caused a concentration-dependent prolongation of the lifetime of PYP_M, we further examined the concentration effects of some other inorganic salts on the decay constant of PYP_M (Fig. 2a). In these experiments 10 mM acetate was present in the solution as buffer (pH 5.0). The decay constant of PYP_M was estimated from the absorbance decrease at 350 nm after shutting off the excitation light. Every decay curve can be fitted to a single exponential curve (Fig. 1b). The decay rate of PYP_M decreased by increasing the concentration of all salts tested. The rate constants were plotted against ionic strength (Fig. 2b). The three curves were almost superimposable (Fig. 2b), indicating that the lifetime of PYP_M depends on the ionic strength.

The Lifetime of PYP_M in the Presence of Various Organic Acid Molecules—We also examined the effect of organic

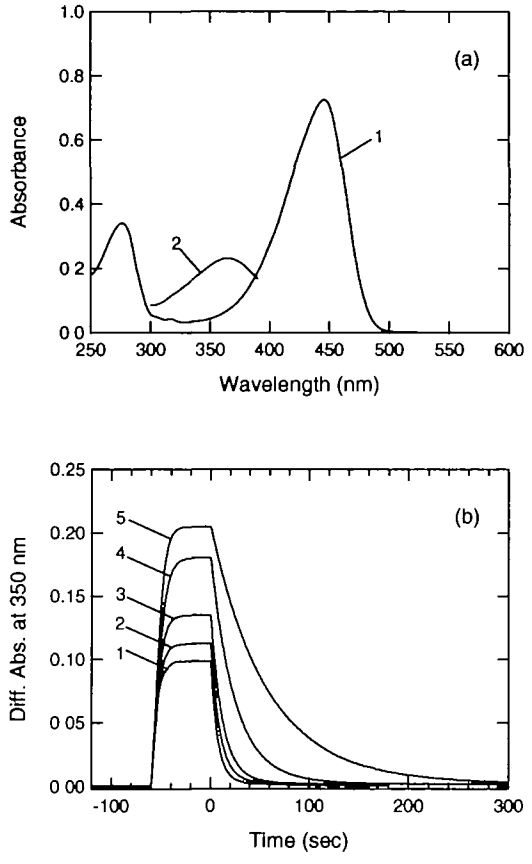

Fig. 1. **(a) Absorption spectra of dark PYP and PYP_M in 300 mM acetate at pH 5.0, 5.0°C.** PYP_M accumulated under continuous illumination (>430 nm). The spectrum of PYP_M was measured using an optical filter to prevent the excitation light from damaging the detector. **(b) Time chart of absorption changes at 350 nm.** The excitation light (>430 nm) was irradiated in the interval (from –60 to 0 s). The curves (1–5) were obtained at various concentration of acetate. 1, 1 mM; 2, 50 mM; 3, 100 mM; 4, 400 mM; 5, 1 M.

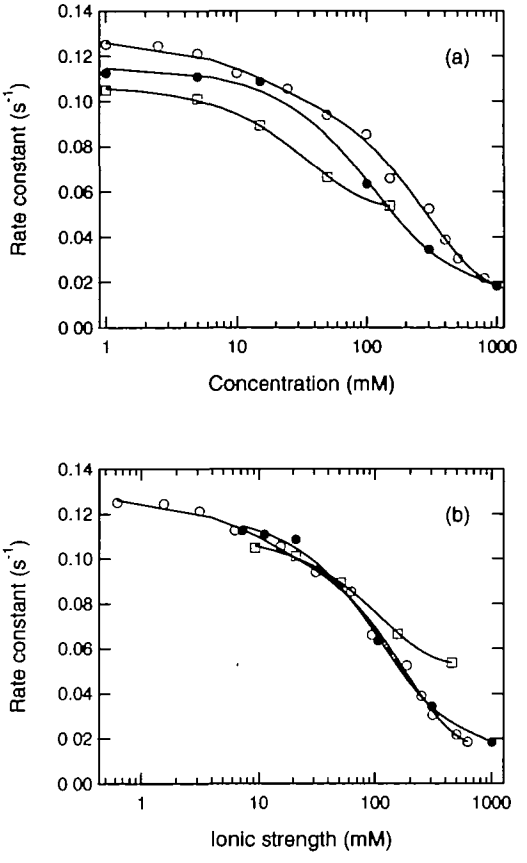

Fig. 2. **(a) The dependence of the decay constant of PYP_M on the concentration of various salts [acetate (○), sodium chloride (●), sodium sulfate (□)]. (b) For the sake of comparison, the *x*-axis represents ionic strength.**

salts other than acetate on the decay rate of PYP_M (Fig. 3a). The concentration effect on the decay rate differed among the organic salts tested. When the rate constant is plotted against the ionic strength, however, the curves do not overlap (Fig. 3b), in a marked contrast to the effects with inorganic salts shown in Fig. 2b. Prolongation of the decay rate took place in the order of citrate, 1,2,3-propane-tricarboxylate, glutarate, and acetate. These results suggest that, in the case of organic salts, the molecular properties also affect the prolongation of PYP_M in addition to the effect of ionic strength.

The Effect of Citrate on the Absorption Spectrum of PYP_M—The spectra of PYP and PYP_M were measured in acetate and in citrate to characterize further the effects of these salts on the lifetime properties of PYP_M. At low concentrations (1 mM citrate and 10 mM acetate), in which the lifetime of PYP_M is comparable to that in the absence of salts, no significant difference in the spectra of PYP and PYP_M were observed between acetate and citrate (Fig. 4, a and b). The spectrum of PYP was independent of the concentration of acetate and citrate (Fig. 4a). Therefore, these salts do not affect the chromophore environment of dark-state PYP. In contrast, a remarkable difference was observed for the PYP_M spectrum between acetate and citrate at higher salt concentrations. Figure 4, c and d, shows the difference absorption spectra for PYP_M in the presence of various concentrations of acetate and citrate, respectively. From these figures it is clear that the spectral changes with citrate are different from those with acetate. The existence of the isosbestic point at 386 nm in acetate suggests a two-state transition from PYP to PYP_M. The spectral shape of PYP_M in acetate is independent of concentration, even though the amount of PYP_M changed due to the difference in lifetime. In the case of citrate, a distinct feature was the lack of a clear isosbestic point (Fig. 4d). This means that PYP_M in citrate buffer comprises multiple species. The λ_{max} of PYP_M blue-shifted from 360 to 350 nm as the concentration of citrate increased, and a shoulder at 330 nm was prominent at concentrations higher than 50 mM. These results suggest that citrate affects the chromophore environment of PYP_M at high concentration. In the present data, each spectrum in Fig. 4d can be reproduced by a linear combination of two typical curves: the difference spectrum of the lowest concentration and that of the highest concentration. This result suggests that these two components for PYP_M are enough to explain the present spectroscopic data. Thus, at least two states of PYP_M are present. One is observed with acetate and at low concentrations of citrate, and the other is observed at high concentrations of citrate.

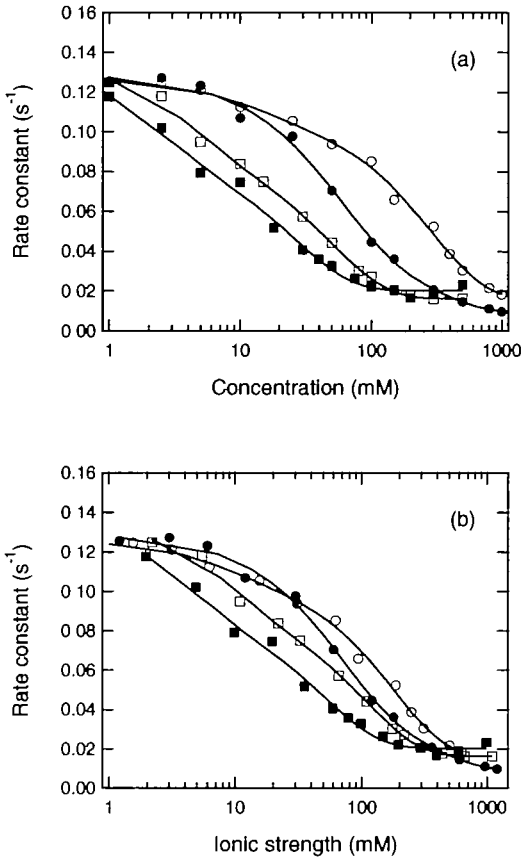

Fig. 3. **(a) The dependence of the decay constant of PYP_M on the concentration of various salts [acetate (○), glutarate (●), 1,2,3-propane-tricarboxylate (□), and citrate (■)]. (b) For the sake of comparison, the *x*-axis represents ionic strength.**

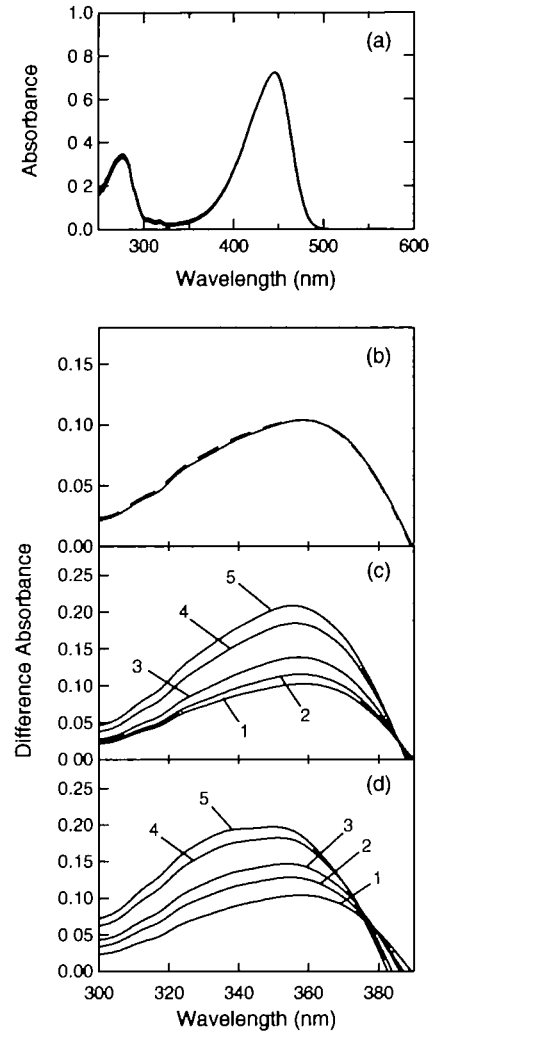

Fig. 4. **(a) Absorption spectra of dark PYP in acetate solution (10 and 300 mM) and citrate solution (1 and 50 mM).** All spectra are superimposed. **(b) Difference in the absorption spectra of PYP_M in 10 mM acetate solution (solid line) and 1 mM citrate solution (dashed line). Difference absorption spectra for PYPM at various concentrations of acetate (c) and citrate (d), where the intensity of excitation light and the concentration of PYP were fixed.** (c) 1, 10 mM; 2, 50 mM; 3, 100 mM; 4, 400 mM; 5, 1 M. (d) 1, 1 mM; 2, 5 mM; 3, 10 mM; 4, 50 mM; 5, 300 mM. The baseline for each spectrum was the corresponding absorption spectrum of each dark state.

The PYP_M observed at higher concentrations of citrate is hereafter called PYP_M'.

Solution Structures of PYP_M and PYP_M' as Determined Using Solution X-Ray Scattering—The solution structures of PYP_M and PYP_M' were characterized by solution X-ray scattering. PYP was suspended in 10 mM acetate buffer, 100 mM acetate buffer, 1 mM citrate buffer, and 50 mM citrate buffer, at pH 5.0 and 5°C. Solution X-ray scattering measurements were carried out with and without illumination.

Figure 5 shows the Guinier plots for PYP and PYP_M in 10 mM acetate buffer (a) and in 50 mM citrate buffer (b) at pH 5.0 and 5°C. The protein concentrations were 4, 6, 8, 10, and 12 mg/ml, from bottom to top. PYP_M accumulated sufficiently under illumination (>95%). For each concentration, PYP_M gave a steeper line than PYP in both acetate and citrate buffer. These results indicate that the radius of gyration (*Rg*) increases upon illumination. Thus, PYP_M is considered to be swollen upon illumination compared to the dark state independent of the buffer system.

The intrinsic values of *Rg* and $I(0)/c$ were obtained by extrapolation to a concentration of zero (Table II). The *Rg* values of the dark state are 15.2 ± 0.2 Å, and independent of the solvent conditions. Since *Rg* is increased by illumination under all solvent conditions, we conclude that PYP is swollen upon the formation of PYP_M. Further, the *Rg* values of PYP_M vary from 15.5 to 16.2 ± 0.3 Å dependent of solvent conditions. The increase in *Rg* in high concentrations of citrate is larger than that under other conditions, indicating that the *Rg* of PYP_M' is larger than that of PYP_M. It should be noted that, at 50 mM citrate, $[I(0)/c]_{conc\to 0}$ of PYP_M' is about 7% larger than that of PYP. The increase of $I(0)/c$ was observed in Guinier plots (Fig. 5b). Although the *y*-intersection was unchanged in 10 mM acetate buffer, the value of the *y*-intersection of PYP_M' was slightly higher than that of PYP in 50 mM citrate buffer. Since protein conformational changes do not cause changes in molecular weight, $[I(0)/c]_{conc\to 0}$ should remain constant. The increase in $I(0)/c$ for PYP_M' is, thus, interpreted as the binding of citrate molecules to PYP_M. As the molecular weight of PYP is

14 kDa, the increase is equivalent to the binding of 4–5 citrate molecules (M.W. 210). Solution X-ray scattering demonstrates that PYP_M' that accumulates at high concentrations of citrate has a different shape and size than PYP_M.

DISCUSSION

The lifetime of PYP_M is prolonged as the concentrations of acetate, sodium chloride, and sodium sulfate are increased. However, the ionic strength dependencies of the decay constants are identical. Under these conditions, the absorption spectra of both PYP and PYP_M exhibit no ionic concentration dependencies.

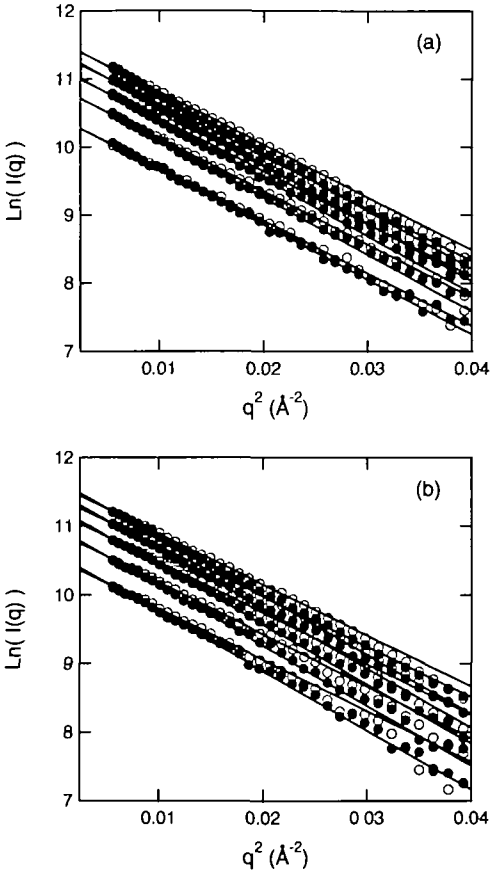

Fig. 5. **Guinier plots for dark PYP (○) and PYP_M (●) at 10 mM acetate (a) and 50 mM citrate (b), pH 5.** Each plot shows data obtained at 4, 6, 8, 10, 12 mg/ml PYP in order from the bottom. X-ray scattering profiles of PYP and PYP_M, measured using the same stock sample.

However, glutarate, 1,2,3-propane-tricarboxylate and citrate all produce another effect in addition to the ionic strength effect. The lifetime of PYP_M is prolonged in increasing order in the presence of glutarate, 1,2,3-propane-tricarboxylate, and citrate. The ionic strength dependencies on the rate constant differ (Fig. 3b), and are completely different from those in the presence of inorganic salts (Fig. 2b). The spectra of PYP_M' obtained at high concentrations of organic ions are different from those of PYP_M, suggesting that these organic acid molecules affect the microenvironment of the chromophore. SAXS measurements revealed a molecular weight increase during PYP_M' formation. Neither the absorption spectra nor X-ray scattering profiles are affected by any solute condition in the dark. Therefore, we consider that the lifetime of PYP_M is further prolonged by conversion to PYP_M' with specific binding of organic acid molecules. The stabilization of PYP_M against urea in citrate buffer, as shown in our previous study (*31*), is, thus, considered to be mediated by citrate binding to PYP_M.

We observed the swelling of the protein structure during PYP_M formation, with an increase in *Rg* of about 0.4 Å. A previous crystallographic study of PYP_M showed that the structural changes are very small and confined to the vicinity of the choromophore. The calculated *Rg* values for the crystalline structures of PYP and PYP_M (2pyp.pdb) are identical (14.5 Å). The calculated value is slightly smaller than the observed values (15.2 Å in the dark), which is understood to represent the contribution of hydration (*37–39*). Although the crystal structure does not suggest that *Rg* increases upon PYP_M formation, the present SAXS experiment clearly shows the increase in *Rg*, suggesting that the PYP_M structure in solution is different from the crystal structure. The discrepancy between the solution structure and the crystalline structure of PYP_M has been observed by various techniques including NMR (*24, 25*), and thermodynamic (*15, 26*) and FTIR studies (*27–29*). We consider that the force constraint of a crystalline lattice suppresses large-scale conformational changes.

Extra structural changes were observed in PYP_M', namely, an increase in the *Rg* value to 16.2 Å, which is significantly larger than that of PYP and PYP_M. The increase is partly due to the specific binding of organic acid molecules, as supported by an increase in $I(0)/c$. Differences in the spectroscopic properties and stability against urea between PYP_M and PYP_M' suggest that the structure of PYP_M' may be different from that of PYP_M. A urea unfolding experiment indicated that the major difference between PYP_M and PYP_M' is observed in the *m*-value, the proportional constant for the increase of ΔG_D against urea concentration (*31*). The *m*-value for PYP_M is larger than that for PYP_M'. The *m*-value is interpreted as the difference in the solvent accessible surface area between the native and unfolded

TABLE II. **The radius of gyration and the forward scattering intensity of PYP under dark and light in acetate solution (10 and 100 mM) and citrate solution (1 and 50 mM).** ($c \rightarrow 0$) means extrapolation to concentration of zero. The value in the parenthesis shows the error.

		$Rg(c \rightarrow 0)$ [Å]		$I(0)/c(c \rightarrow 0)$	
		Dark	Light	Dark	Light
Acetate	10 mM	15.2 (0.2)	15.6 (0.3)	9,000 (200)	9,000 (300)
	100 mM	15.2 (0.2)	15.8 (0.2)	9,000 (200)	9,000 (200)
Citrate	1 mM	15.1 (0.2)	15.5 (0.2)	8,800 (200)	8,800 (300)
	50 mM	15.2 (0.2)	16.2 (0.2)	8,900 (100)	9,500 (100)

states (*40*). Therefore, the solvent accessible surface area of PYP_M' in citrate is considered to be larger than that of PYP_M in acetate. Thus, we can expect further structural change at PYP_M' from PYP_M. In the present study, we were able to distinguish two PYP_M states. We suggest that PYP_M in acetate is the state capable of target recognition and PYP_M' in citrate is the target-bound state.

The mid-concentration of the kinetics changes decreases in the order of acetate, glutarate, 1,2,3-propane-tricarboxylate, and citrate, suggesting that the binding affinity of these ions should increase in this order except for acetate. Note that acetate does not bind to PYP. These organic molecules can possess the same number of negative charges as the number of carboxyl groups they contain, *i.e.*, 1 for acetate, 2 for glutarate, and 3 for 1,2,3-propane-tricarboxylate and citrate. The effects of inorganic salts clearly indicate that the number of electrical charges is not responsible for the specific interaction of ionic molecules with PYP. Therefore, a property other than the number of electrical charges determines the formation of PYP_M'.

Citrate is widely used to crystallize proteins under acidic conditions, and thus many crystal structures coordinated with citrate molecules have been registered on PDB. In some cases, citrate is specifically bound to a protein *via* hydrogen bonds (*41–43*). The crystal structure of the RNA 3′ terminal phosphate cyclase is a typical case (*41*). In this protein, the citrate molecule interacts simultaneously with several basic residues through hydrogen bonds. The basic residues are spatially separated from each other on the surface of the protein and constitute a cluster. Such a cluster of basic residues may explain the difference in the binding stability to PYP_M between acetate, glutarate, 1,2,3-propane-tricarboxylate, and citrate. All these weak acids contain carboxyl group(s) and can be bound to a cluster of basic residues similar to citrate. The numbers of possible hydrogen bonding sites are 2 for acetate, 4 for glutarate, 6 for 1,2,3-propane-tricarboxylate, and 7 for citrate. Therefore, the binding stability could be related to the number of sites for hydrogen bonds between the acid and protein. This would then give a binding stability in increasing order of acetate, glutarate, 1,2,3-propane-tricarboxylate, and citrate. Sulfate ions cannot interact with proteins because the distance between the charges is much smaller than that of glutarate despite the fact that sulfate has the same number of hydrogen bond acceptor sites as glutarate. Previous crystallographic studies on PYP_M proposed that the only change on the protein surface is the exposure of Arg52 to solvent (*4*). To deduce about the citrate-binding cluster composed of basic residues, we carefully searched in the vicinity of Arg52 using the crystal structures of PYP and PYP_M (2pyp.pdb) (*4*). Although such a cluster cannot be seen in the dark state, the exposure of Arg52 on PYP_M generates a cluster with a size similar to a citrate molecule, which is composed of Arg52, Lys60 at the edge of β3 and Tyr98, Glu99 on loop β4 and β5 (Fig. 6). The cluster composed of Arg52 and some amino acid residues proposed here are the putative interactive sites in PYP_M under physiological conditions. However, Arg52 is not conserved in other PAS domain sequences. Therefore, the exposure of the cluster of positive charges observed in PYP may not be a common event among PAS family members. This hypothesis merits further study. In order to elucidate candidate residues of the target binding site, we are investigating the citrate binding area on PYP_M using a site-directed mutant of PYP.

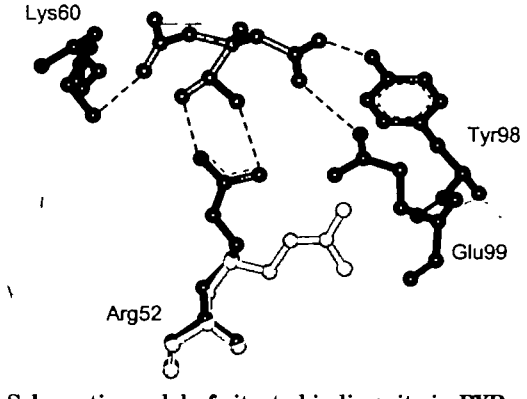

Fig. 6. **Schematic model of citrate binding site in PYP_M, based on the crystal structure previously reported (PDB ID: 2PYP, *4*).** A citrate molecule and the residues bound to the citrate molecule *via* hydrogen bonding are represented by a ball-and-stick model. Two conformations shown as black and white are superimposed at Arg52, and represent the conformation of Arg52 in PYP_M and that in the dark-state, respectively.

The experiments at Photon Factory BL-10C were performed under the approval of the Photon Factory Advisory Committee (Proposal No. 98G191 and 2000G162).

REFERENCES

1. Meyer, T.E. (1985) Isolation and characterization of soluble cytochromes, ferredoxins and other chromophoric proteins from the halophilic phototrophic bacterium *Ectothiorhodospira halophila*. *Biochim. Biophys. Acta* **806**, 175–183
2. Sprenger, W.W., Hoff, W.D., Armitage, J.P., and Hellingwerf, K.J. (1993) The eubacterium *Ectothiorhodospira halophila* is negatively phototactic, with a wavelength dependence that fits the absorption spectrum of the photoactive yellow protein. *J. Bacteriol.* **175**, 3096–3104
3. Borgstahl, G.E.O., Williams, D.R., and Getzoff, E.D. (1995) 1.4 Å structure of photoactive yellow protein, a cytosolic photoreceptor: unusual fold, active site, and chromophore. *Biochemistry* **34**, 6278–6287
4. Genick, U.K., Borgstahl, G.E., Ng, K., Ren, Z., Pradervand, C., Burke, P.M., Srajer, V., Teng, T.Y., Schildkamp, W., McRee, D.E., Moffat, K., and Getzoff, E.D. (1997) Structure of a protein photocycle intermediate by millisecond time-resolved crystallography. *Science* **275**, 1471–1475
5. Genick, U.K., Soltis, S.M., Kuhn, P., Canestrelli, I.L., and Getzoff, E.D. (1998) Structure at 0.85 Å resolution of an early protein photocycle intermediate. *Nature* **392**, 206–209
6. Perman, B., Šrajer, V., Ren, Z., Teng, T., Pradervand, C., Ursby, T., Bourgeois, D., Schotte, F., Wulff, M., Kort, R., Hellingwerf, K., and Moffat, K. (1998) Energy transduction on the nanosecond time scale: early structural events in a xanthopsin photocycle. *Science* **279**, 1946–1950
7. Pellequer, J.-L., Wager-Smith, K.A., Kay, S.A., and Getzoff, E.D. (1998) Photoactive yellow protein: a structural prototype for the three-dimensional fold of the PAS domain superfamily. *Proc. Natl. Acad. Sci. USA* **95**, 15177–15182
8. Cabral, J.H.M., Lee, A., Cohen, S.L., Chait, B.T., Li, M., and Mackinnon, R. (1998) Crystal structure and functional analysis of the HERG potassium channel N terminus: a eukaryotic PAS domain. *Cell* **95**, 649–655
9. Gong, W., Hao, B., Mansy, S.S., Gonzalez, G., Gilles-Gonzalez, M.A., and Chan, M.K. (1998) Structure of a biological oxygen sensor: a new mechanism for heme-driven signal transduction.

Proc. Natl. Acad. Sci. USA **95**, 15177–15182
10. Van Aalten, D., Crielaard, W., Hellingwerf, K.J., and Joshua-Tor, L. (2000) Conformational substrates in different crystal forms of the photoactive yellow protein—correlation with theoretical and experimental flexibility. *Protein Sci.* **9**, 64–72
11. Hoff, W.D., Düx, P., Hård, K., Devreese, B., Nugteren-Roodzant, I.M., Crielaard, W., Boelens, R., Kaptein, R., Van Beeumen, J., and Hellingwerf, K.J. (1994) Thiol ester-linked *p*-coumaric acid as a new photoactive prosthetic group in a protein with rhodopsin-like photochemistry. *Biochemistry* **33**, 13959–13962
12. Baca, M., Borgstahl, G.E.O., Boissinot, M., Burke, P.M., Williams, D.R., Slater, K.A., and Getzoff, E.D. (1994) Complete chemical structure of photoactive yellow protein: novel thioester-linked 4-hydroxycinnamyl chromophore and photocycle chemistry. *Biochemistry* **33**, 14369–14377
13. Imamoto, Y., Ito, T., Kataoka, M., and Tokunaga, F. (1995) Reconstitution photoactive yellow protein from apoprotein and *p*-coumaric acid derivatives. *FEBS Lett.* **374**, 157–160
14. Meyer, T.E., Yakali, E., Cusanovich, M.A., and Tollin, G. (1987) Properties of a water-soluble, yellow protein isolated from a halophilic phototrophic bacterium that has photochemical activity analogous to sensory rhodopsin. *Biochemistry* **26**, 418–423
15. Meyer, T.E., Tollin, G., Hazzard, J.H., and Cusanovich, M.A. (1989) Photoactive yellow protein from the purple phototrophic bacterium, *Ectothiorhodospira halophila*. Quantum yield of photobleaching and effects of temperature, alcohols, glycerol, and sucrose on kinetics of photobleaching and recovery. *Biophys. J.* **56**, 559–564
16. Hoff, W.D., Kwa, S.L.S., Van Grondelle, R., and Hellingwerf, K.J. (1992) Low temperature absorbance and fluorescence spectroscopy of the photoactive yellow protein from *Ectothiorhodospira halophila*. *Photochem. Photobiol.* **56**, 529–539
17. Hoff, W.D., Van Stokkum, I.H.M., Van Ramesdonk, H.J., Van Brederode, M.E., Brouwer, A.M., Fitch, J.C., Meyer, T.E., Van Grondelle, R., and Hellingwerf, K.J. (1994) Measurement and global analysis of the absorbance changes in the photocycle of the photoactive yellow protein from *Ectothiorhodospira halophila*. *Biophys. J.* **67**, 1691–1705
18. Chosrowjan, H., Mataga, N., Nakashima, N., Imamoto, Y., and Tokunaga, F. (1997) Femtosecond-picosecond fluorescence studies on excited state dynamics of photoactive yellow protein from *Ectothiorhodospira halophila*. *Chem. Phys. Lett.* **270**, 267–272
19. Ujj, L., Devanathan, S., Meyer, T.E., Cusanovich, M.A., Tollin, G., and Atkinson, G.H. (1998) New photocycle intermediates in the photoactive yellow protein from *Ectothiorhodospira halophila*: picosecond transient absorption spectroscopy. *Biophys. J.* **75**, 406–412
20. Imamoto, Y., Kataoka, M., Tokunaga, F., Asahi, T., and Masuhara, H. (2001) Primary photoreaction of photoactive yellow protein studied by subpicosecond-nanosecond spectroscopy. *Biochemistry* **40**, 6047–6052
21. Imamoto, Y., Kataoka, M., and Tokunaga, F. (1996) Photoreaction cycle of photoactive yellow protein from *Ectothiorhodospira halophila* studied by low-temperature spectroscopy. *Biochemistry* **35**, 14047–14053
22. Imamoto, Y., Mihara, K., Hisatomi, O., Kataoka, M., Tokunaga, F., Bojkova, N., and Yoshihara, K. (1997) Evidence for proton transfer from Glu-46 to the chromophore during the photocycle of photoactive yellow protein. *J. Biol. Chem.* **272**, 12905–12908
23. Xie, A., Hoff, W.D., Kroon, A.R., and Hellingwerf, K.J. (1996) Glu46 donates a proton to the 4-hydroxycinnamate anion chromophore during the photocycle of photoactive yellow protein. *Biochemistry* **35**, 14671–14678
24. Rubinstenn, G., Vuister, G.W., Mulder, F.A., Dux, P.E., Boelens, R., Hellingwerf, K.J., and Kaptein, R. (1998) Structural and dynamic changes of photoactive yellow protein during its photocycle in solution. *Nat. Struct. Biol.* **5**, 568–570
25. Craven, C.J., Derix, N.M., Hendriks, J., Boelens, R., Hellingwerf, K.J., and Kaptein, R. (2000) Probing the nature of the blue-shifted intermediate of photoactive yellow protein in solution by NMR: hydrogen-deuterium exchange data and pH studies. *Biochemistry* **39**, 14392–14399
26. Van Brederode, M.E., Hoff, W.D., Van Stokkum, I.H.M., Groot, M.-L., and Hellingwerf, K.J. (1996) Protein folding thermodynamics applied to the photocycle of the photoactive yellow protein. *Biophys. J.* **71**, 365–380
27. Hoff, W.D., Xie, A., Van Stokkum, I.H., Tang, X.J., Gural, J., Kroon, A.R., and Hellingwerf, K.J. (1999) Global conformational changes upon receptor stimulation in photoactive yellow protein. *Biochemistry* **38**, 1009–1017
28. Kandori, H., Iwata, T., Hendriks, J., Maeda, A., and Hellingwerf, K.J. (2000) Water structural changes involved in the activation process of photoactive yellow protein. *Biochemistry* **39**, 7902–7909
29. Xie, A., Kelemen, L., Hendriks, J., White, B.J., Hellingwerf, K.J., and Hoff, W.D. (2001) Formation of a new buried charge drives a large-amplitude protein quake in photoreceptor activation. *Biochemistry* **40**, 1510–1517
30. Brudler, R., Rammelsberg, R., Woo, T.T., Getzoff, E.D., and Gerwert, K. (2001) Structure of the I1 early intermediate of photoactive yellow protein by FTIR spectroscopy. *Nat. Struct. Biol.* **8**, 265–270
31. Ohishi, S., Shimizu, N., Mihara, K., Imamoto, Y., and Kataoka, M. (2001) Light induces destabilization of photoactive yellow protein. *Biochemistry* **40**, 2854–2859
32. Mihara, K., Hisatomi, O., Imamoto, Y., Kataoka, M., and Tokunaga, F. (1997) Functional expression and site-directed mutagenesis of photoactive yellow protein. *J. Biochem.* **121**, 876–880
33. Ueki, T., Hiragi, Y., Kataoka, M., Inoko, Y., Amemiya, Y., Izumi, Y., Tagawa, H., and Muraga, Y. (1985) Aggregation of bovine serum albumin upon cleavage of its disulfide bonds, studied by the time-resolved small-angle X-ray scattering technique with synchrotron radiation. *Biophys. Chem.* **23**, 115–123
34. Kataoka, M., Head, J.F., Persechini, A., Kretsinger, R.H., and Engleman, D.M. (1991) Small-angle X-ray scattering studies of calmodulin mutants with deletions in the linker region of the central helix indicate that the linker region retains a predominantly alpha-helical conformation. *Biochemistry* **30**, 1188–1192
35. Guinier, A. and Fournet, G. (1955) *Small Angle X-Ray Scattering*, John-Wiley and Sons, New York
36. Glatter, O. and Kratky, O. (1982) *Small Angle X-Ray Scattering*, Academic Press, New York
37. Fujisawa, T., Uruga, T., Yamaizumi, Z., Inoko, Y., Nishimura, S., and Ueki, T. (1994) The hydration of Ras p21 in solution during GTP hydrolysis based on solution X-ray scattering profile. *J. Biochem.* **1155**, 875–880
38. Svergun, D.I., Barberato, C., and Koch, M.H.J. (1995) CRYSOL—a program to evaluate X-ray solution scattering of biological macromolecules from atomic coordinates. *J. Appl. Crystallogr.* **28**, 768–773
39. Svergun, D.I., Richard, S., Koch, M.H.J., Sayers, Z., Kuprin, S., and Zaccai, G. (1998) Protein hydration in solution: experimental observation by x-ray and neutron scattering. *Proc. Natl. Acad. Sci. USA* **95**, 2267–2272
40. Schellman, J.A. (1978) Solvent denaturation. *Biopolymers* **17**, 1305–1322
41. Palm, G.J., Billy, E., Filipowicz, W., and Wlodawer, A. (2000) Crystal structure of RNA 3′-terminal phosphate cyclase, a ubiquitous enzyme with unusual topology. *Structure* **8**, 13–23
42. Harrison, D.H., Bohren, K.M., Petsko, G.A., Ringe, D., and Gabbay, K.H. (1997) The alrestatin double-decker: binding of two inhibitor molecules to human aldose reductase reveals a new specificity determinant. *Biochemistry* **36**, 16134–16140
43. Abad-Zapatero, C., Griffith, J.P., Sussman, J.L., and Rossmann, M.G. (1987) Refined crystal structure of dogfish M4 apo-lactate dehydrogenase. *J. Mol. Biol.* **198**, 445–467